Distribution Agreement

In presenting this thesis as a partial fulfillment of the requirements for a degree from Emory University, I hereby grant to Emory University and its agents the non-exclusive license to archive, make accessible, and display my thesis in whole or in part in all forms of media, now or hereafter now, including display on the World Wide Web. I understand that I may select some access restrictions as part of the online submission of this thesis. I retain all ownership rights to the copyright of the thesis. I also retain the right to use in future works (such as articles or books) all or part of this thesis.

Ashley Oldshue April 9, 2019

Modeling history-dependent cross-bridge dynamics for force generation in a muscle unit

by

Ashley Oldshue

Lena H. Ting
Adviser

Neuroscience and Behavioral Biology

Lena H. Ting

Adviser

Samuel J. Sober

Committee Member

Trisha M. Kesar

Committee Member

Gregory S. Sawicki

Committee Member

2019

Modeling history-dependent cross-bridge dynamics for force generation in a muscle unit

By

Ashley Oldshue

Lena H. Ting

Adviser

An abstract of
a thesis submitted to the Faculty of Emory College of Arts and Sciences
of Emory University in partial fulfillment
of the requirements of the degree of
Bachelor of Sciences with Honors

Neuroscience and Behavioral Biology

2019

Abstract

Modeling history-dependent cross-bridge dynamics for force generation in a muscle unit
By Ashley Oldshue

Muscles exhibit history-dependent and transient behaviors during movement. However, the mechanisms of force production that respond to prior movement and activation remain unclear. Existing muscle models, such as the Hill-type model of contraction dynamics, have encompassed important behaviors under static conditions by using experimental results to govern the kinematic responses of the model. However, these force-length and force-velocity relationships are not always generalizable to forces generated during movement. Muscle models have yet to incorporate physiological mechanisms of contraction dynamics on the filament level. The interfilamentary cross-bridge interactions between actin binding sites and cycling myosin heads are thought to be responsible for history-dependent behaviors, such as short-range stiffness that produces an increased initial force response to an imposed stretch. By modeling the cross-bridge dynamics of a muscle unit, we are able to incorporate key features of force generation during dynamic movements. Our model consists of a two-state cross-bridge system, governed by activation dynamics and the position and time dependent cycling behavior of the myosin heads. Initial simulations confirmed that the short-range stiffness and rapid transient responses of the model are similar to previous simulation results as well as filament level experimental results. These simulations verified that the force behaviors were consistent with cross-bridge mechanisms and exhibited history-dependent responses. We then performed force-length and force-velocity tests to characterize the emergent steady state properties of the model. The cross-bridge model was able to intrinsically produce length and velocity dependent forces under static conditions consistent with experimental results used in Hill-type models. By defining these behaviors, the model has the potential to be applied to dynamic movement simulations. History-dependence is thought to be a major contributor to locomotive strategies needed for navigating unpredictable environments, such as reacting to unexpected ground forces. Modeling the muscle properties that contribute to robust behaviors in complex environments may allow us to understand the mechanisms of movement, and movement control, in healthy and impaired systems.

Modeling history-dependent cross-bridge dynamics for force generation in a muscle unit

By

Ashley Oldshue

Lena H. Ting

Adviser

A thesis submitted to the Faculty of Emory College of Arts and Sciences
of Emory University in partial fulfillment
of the requirements of the degree of
Bachelor of Sciences with Honors

Neuroscience and Behavioral Biology

2019

Acknowledgements

First and foremost, I want to sincerely thank my research advisor, Dr. Lena H. Ting. Dr. Ting has been an extraordinary teacher and mentor to me. From the moment she allowed me to join her lab sophomore year, all the way through the faith she put in me for this project, she has gone above and beyond to invest time, energy, and resources into helping me reach my research goals. She has far surpassed any expectations I had and has continuously challenged me to push myself. Her ambition, dedication, and leadership are what I aim to embody in my career, and I cannot thank her enough for allowing me to be a part of her lab and see the quality of work and thought that goes on there first hand.

Secondly, I would like to thank my committee members Dr. Samuel J. Sober, Dr. Trisha M. Kesar, and Dr. Gregory S. Sawicki. I am so grateful to have had the support and contributions of such incredible researchers and mentors. Their continued interest and input for this project is what allowed it to come to fruition. Furthermore, their investment has made the entire experience rewarding and educational, as well as enjoyable.

Thirdly, I want to acknowledge the influence of my rotation with the Power Lab at the Georgia Institute of Technology. Dr. Sawicki and all of his lab members have helped me take my abstract ideas and research goals and turn them into concrete work. Specifically, Laksh K. Punith who invested countless hours, not only in this project, but in helping me expand my research and education in computational and engineering techniques.

Finally, I want to thank all the members of the Neuromechanics Lab at Emory that have helped me develop into the researcher I am today. Being a part of a collaborative, inclusive, and interdisciplinary lab is one of my most valued experiences at Emory. In particular, Dr. Aiden Payne who took innumerable amounts of time out of his own Ph.D. work to mentor me and help me develop independent research goals. I owe much of this project, as well as every other opportunity I have received that has come out of being involved in the Neuromechanics Lab, to him and his constant support.

Table of Contents

Figures

INTRODUCTION

The exploration of biomechanics through experimental methods and modeling techniques is extensive. However, the mechanisms of generating movement have yet to be clearly defined. While we are able to discretely quantify the behaviors produced in movement and balance conditions, the underlying biomechanical systems are poorly understood. Behaviors ranging from simple contractions to complex, multi-joint movements, as well as the neural signals that control them, are dependent on the mechanical properties of the muscles and tendons. Therefore, the physical properties of these biological systems determine the patterns of force generation during movement. The difficulty in defining such parameters is that muscle physiology does not produce static behaviors, but instead allows for flexible and highly robust responses. Models that rely on experimental data alone tend to ignore the biomechanical properties that govern muscle behaviors and produce rigid force generation patterns that do not apply to complex actions. Transient and history-dependent properties of skeletal muscle behaviors may have important effects in the control and execution of dynamic movements, including unpredictable interactions with the environment. Complex movements in real-life environments require not only forces that produce the actions themselves, but also the ability to navigate uneven terrain and react to unexpected external forces. The biomechanical mechanisms that govern such responses have yet to be determined (Voloshina, Kuo, Daley, & Ferris, 2013). Simulating simple muscle systems with more biologically accurate features is the next step in the ability to understand, test, and correct locomotion strategies in humans.

Muscle Physiology

The muscle-tendon unit is the link between the central nervous system and behavior. Skeletal muscles are activated through electrical impulses to generate force, which acts on the

skeleton through tendons. This allows the body to maintain upright posture and balance, as well as produce actions from eye movements to locomotion (Zajac, 1989). The connective tissue of the tendons is continuous and extends around the force-generating body of the muscle. Connective tissue within the muscle forms fascicles that bundle together hundreds to thousands of parallel muscle fibers. Each muscle fiber runs the entire length of the muscle and is innervated by motor neurons. This is the connection to the central nervous system that allows for neural control of movement and behavior. Motor neurons have some of the largest diameter axons in the nervous system, which allows action potentials to propagate at high velocities and for neural signals to reach muscles quickly. Every muscle fiber is controlled by a single motor neuron. However, motor neurons control many muscle fibers, which determines the strength of contraction. When an action potential is triggered in a motor neuron, every fiber it innervates contracts, producing force in the muscle (Stanfield, 2017).

Muscle fibers themselves are comprised of base contractile elements, sarcomeres, which are connected in series to allow for shortening of the entire muscle. A sarcomere consists of a thick and thin filament made of myosin and actin proteins, respectively. These proteins can bind and exert a sideways force that allows the parallel filaments to slide past each other. As the filaments slide, the ends of the sarcomere are drawn closer together. The simultaneous shortening of the sarcomeres in a muscle fiber is known as the sliding filament theory, which allows muscle contraction to occur (Stanfield, 2017).

The ability of the sarcomere to shorten is dependent on both the activation of the actin binding sites on the thin filament and the cycling activity of the myosin heads on the thick filament. Chemical changes due to muscle activation lead to conformational changes on the thin filament that exposes the binding sites (Campbell, 2014). The myosin heads operate in a

multiple state system in which some states are available for binding and some are not. When the myosin moves into the "cocked" position through a chemical process that releases energy, it can then attach to the available actin sites, form a cross-bridge, and generate a force through a subsequent conformational change called a power stroke (Stanfield, 2017). The cycling activity between the different myosin head states is dependent on the rates of attachment and detachment (Blum, 2018).

Cross-bridge dynamics

The mechanisms of cross-bridge behavior are thought to be responsible for history-dependence in muscles. When a muscle is stretched after a period of being held isometrically, the tension response is biphasic, featuring a steep initial rise followed by a more gradual response (Campbell & Lakie, 1998; Proske & Morgan, 1999; Rack & Westbury, 1974). Besides the initial burst, the tension response is governed by the length change of the muscle and velocity of the imposed stretch (Zajac, 1989). This phenomenon is referred to as short-range stiffness, a key component of history-dependence as it is dependent on recent prior movement and activation within the muscle (Blum, 2018). The high transient forces produced after a muscle is at rest has been attributed to the attachment and detachment activity of the cross-bridges. When a muscle is held isometrically, cross-bridge attachments are allowed to reform, stabilizing the connections between the thick and thin filaments. Initial phases of the tension response to an imposed stretch is thought to be due to the high proportion of attached cross-bridges that resist stretch before beginning to detach (Rack & Westbury, 1974; Proske & Morgan, 1999). Prior movement reduces this stiffness response, implying that the initial segment is determined by the amount of time at rest and the latter portion is primarily a response to stretch velocity (Campbell & Lakie, 1998).

Muscle behaviors

The dynamics of skeletal muscle force during isometric and isotonic contractions produce characteristic force-length and force-velocity relationships, respectively (McMahon, 1984). Force-length measurements are obtained experimentally by fixing the muscle at given lengths and applying an activation, producing an isometric contraction where the length does not change. The active force peaks at some optimal length for the muscle and declines when the muscle is held at lengths greater than optimal. This force also falls when the muscle is held at lengths below this point, slowly at first and more steeply as lengths continue to decrease (McMahon, 1984; Rack & Westbury, 1969; Zajac, 1989). This force-length relationship is consistent across the entire muscle as well as single fiber preparations, where different segments of the curve correspond with different phases of overlap at the filament level. This suggests that the tension produced in the classic force-length experiments is dependent on cross-bridge dynamics because the amount of overlap between filaments is what allows for the cross-bridge force to develop (McMahon, 1984). It is due to the homogeneous arrangement of muscle tissue that the functional properties are carried over from sarcomeres to fibers and entire motor units, excluding differences of scale (Zajac, 1989).

The passive force is generated through elasticity of the muscle tissue and thus responds to length changes independent from the activation dynamics. Passive force is generated at lengths greater than or equal to the optimal muscle length. The total force of the muscle contraction is the sum of both the active and passive components. Therefore, the total force follows the active force curve at lengths below optimal, but will continue to increase as the passive force continues to rise at greater lengths (Zajac, 1989). The composition and structure of different muscles, such

as pennate muscles with more connective tissue, produce different scales of passive force that change the shape of the total force curve (McMahon, 1984).

An isotonic contraction is when a muscle under tension is activated and experiences a contraction. The muscle shortens and then stops once it reaches a stable length and force. The force is taken during the lengthening or shortening movement to measure the force-velocity relationship. This curve reflects a maximum force produced at high lengthening velocities and a maximum shortening velocity before the muscle force falls to zero. Force velocity relationships are used in simulations of muscle behavior under the assumption that the slope of the force-velocity curve is continuous through zero velocity and that the overall relationship is unaffected by prior events. However, the understanding of cross-bridge dynamics and history dependence in real muscles contradict both of these conditions (Zajac, 1989).

Existing models

Through a modeling approach, we are able to simplify the set of tested parameters and isolate specific mechanisms responsible for producing muscle behaviors. Comparing different models allows us to examine the capabilities and limitations of each in explaining the kinematic features of force generation in static conditions and dynamic movements.

Models thus far have been unable to generate accurate measures of muscle activity. Therefore, the information that is being used and the patterns of force production within the muscle, as well as the signals being sent back to the nervous system, are unclear. Being able to reconstruct these dynamic biomechanical systems is critical to understanding not only how healthy individuals navigate their environment, but also conditions of movement disorder or balance impairment.

It has been generally accepted that length, velocity, and activation are the determinants of muscle force outputs. Thus, these have been encoded into most existing muscle unit models, such as the widely used Hill-type model of contraction dynamics. The Hill-type model represents muscle tissue altogether by deriving force from a single contractile unit and a single passive unit in parallel. The contractile unit takes length, velocity, and activation as inputs and calculates an active force according to experimentally determined force-length and force-velocity relationships. The passive unit only responds to length and represents the force produced by the muscle when it is stretched without activation. The total force is a sum of the active and passive forces. This model allows simple integration with a tendon by the addition of a series elastic element to the total muscle unit (Zajac, 1989).

While length, velocity, and activation inputs to the muscle modulate the force output, the physiological mechanisms that take this information, and then undergo intrinsic behaviors to generate internal forces, have been largely ignored. The Hill-type model uses force patterns recorded from static conditions performed under highly controlled experimental conditions in order to deduce force from length and velocity alone. These force relationships are not always applicable to force generated during movement or muscle stretch due to external disturbances (Rack & Westbury, 1969). Therefore, Hill-type models have been poor at predicting forces produced *in vivo* during dynamic tasks that involve transient behaviors and submaximal activation conditions (Dick, Biewener, & Wakeling, 2017). Overall, the functions of Hill-type models are highly rigid and do not incorporate fundamental characteristics of history-dependent muscle behaviors. Thus, many patterns of behavior and sensory feedback cannot be simulated or explained by these models alone.

In order to accurately represent the robustness of locomotion behaviors, muscle models must incorporate the characteristics of muscle physiology that allow for flexible and dynamic responses. A. F. Huxley was one of the first to suggest a model that incorporated the filament-level interactions within muscles. The model included a myosin filament "sliding member" that represented the elastic capabilities of cross-bridge connections. The member oscillates back and forth and may attach or detach to a point on the corresponding actin filament, the rates of which depend on the relative positions of both filaments. Once attachment occurs, tension is produced from the elasticity of the myosin element. The probability of detachment is lowest when the sliding member and actin binding site are aligned, but increases exponentially with displacement in either direction (Huxley, 1957). Modeling capabilities now allow us to more accurately depict large scale cycling myosin activity and cross-bridge dynamics. However, this early design provided key insight into modeling cross-bridge distributions. Another approach has been to model the degree of distortion of each attached cross-bridge, averaged over each possible myosin state (Razumova, Bukatina, & Campbell, 1999). However, modelling the distribution of formed cross-bridges over different attachment lengths allows for increased control of the different kinematic features of myosin behaviors across experimental conditions (Campbell, 2014).

Simulating cross-bridge dynamics has allowed models to exhibit thixotropic stiffness changes (Campbell & Lakie, 1998). Thixotropy refers to the history-dependent property of muscles where forces generated depend on prior movements and activations. This phenomenon, short-range stiffness, is thought to arise from the cycling cross-bridges as it is able to reset over time as the cross-bridges reform (Blum, 2018). It has been suggested that passive components of muscles (i.e. forces generated with no activation in response to imposed stretches) may contribute to history-dependent behaviors (Campbell & Moss, 2002). However, measurements

of length changes during imposed constant velocity stretches in activated muscles show that the sarcomere length temporarily lags behind the imposed length change, due to attached cross-bridges, which causes a brief period of acceleration before the sarcomere reaches a constant stretch velocity. This points to cross-bridge mechanisms as the main contributor to biphasic tension responses in muscles (i.e. short-range stiffness), with the initial steep responses occurring during this period of acceleration (Campbell & Lakie, 1998).

Short-range stiffness is a key component of history-dependent force generation in real muscles that is critical to the study of dynamic movements such as balance perturbations and locomotion. Under any condition where a muscle is stretched more than once, the time interval between the stretches should be a major determining factor of the forces generated. If the stretches occur close together, the forces produced in latter stretches are reduced compared to the initial stretch. If there is a relatively longer time interval between them, the latter stretch response will proceed the same as the initial one (Campbell & Moss, 2002). Cross-bridge models have been able to capture characteristics of these history-dependent behaviors by focusing on the intrinsic cycling activity of the myosin heads that produce forces not only as a function of length, velocity, and activation, but also time (Blum, 2018).

Future Directions

Targeting history-dependence in muscles has the potential to explain patterns of muscle spindle firing rates, a key source of proprioceptive feedback from skeletal muscles (Blum, 2018). It has been found that firing rates vary more directly with force-related variables, than just length and velocity, in reflexive and history-dependent conditions (Blum, D'Incamps, Zytnicki, & Ting, 2017). Therefore, a model that is able to produce history-dependent patterns of force production

should also provide the capability of producing more physiologically precise sensory output signals than a Hill-type model.

The cross-bridge model has yet to be implemented with a tendon as well. The force generated by the muscle in a muscle-tendon unit is influenced by the stiffness or compliance of the tendon. Studying the model with and without a tendon could help define the contributions of cross-bridge elasticity separate from the elasticity of the tendon (Zajac, 1989). It will also provide a system for studying changes in tendon properties and could help explain the energetics of the muscle-tendon unit. Short-range stiffness specifically may contribute to tendon energy storage. When the muscle tension is higher during initial stretches, the length change of the muscle is lower, resulting in greater stretch of the tendon. Since the tendon is modeled as a spring component, greater length changes affect the potential elastic energy stored in the tendon and the forces produced.

The activation dynamics of the Hill-type model are often used to simulate cyclic contractions, which are typical in locomotion (Ross, Nigam, & Wakeling, 2018). Specifically, a simulation of vertical hopping provides a model system for studying the role of neural control in a muscle-tendon unit system. The hopping behaviors, such as height and flight time, are governed by the patterns of activation within the muscle as well as the work done by the elastic components of the muscle-tendon unit to resist a gravitational load (Robertson & Sawicki, 2014). Once integrated, a muscle-tendon unit can be implemented with different load conditions. This allows simulations to be run examining the contributions of assistive and wearable devices, such as exoskeletons (Robertson & Sawicki, 2014).

Most significantly, this approach lends itself to studying perturbations. The hopping model provides a paradigm for studying not only stable, cyclic movements, but the influence of

external disturbances during these behaviors, such as varying the timing of ground reaction forces. History-dependence in muscles is known to cause non-linear behaviors in steady conditions (Campbell & Moss, 2002; Libby, Chukwueke, & Sponberg, 2019). However, recent studies have begun characterizing the effects of history-dependence in perturbed systems. The energetics of the system are largely predictable based on the amount of force within the muscle at the beginning of the perturbation (Libby, Chukwueke, & Sponberg, 2019). Therefore, the ability to map the distribution of cross-bridge attachments over time and incorporate the influence of movement history may be crucial to predicting these behaviors. The cross-bridge muscle model could provide unique insight into the role of history-dependence during these simulations and in the stabilization of cyclic movements following disturbances – an important mechanism of navigating complex environments and uneven terrain.

METHODS

Cross-Bridge Model

The structure of the model that our lab has developed stems from a simplified version of Dr. Kenneth S. Campbell's cross-bridge model, MyoSim, used to study dynamic coupling between activation of actin binding sites and cycling of myosin heads through Calcium signals (Campbell, 2014). The model used for our simulations was developed by Dr. Kyle P. Blum and uses Matlab to simulate a population of cycling cross-bridges in order to generate the force produced by muscle fibers. Specifically, this version consists of a single half sarcomere with a myosin head density of 6.9×10^{16} m^{-2} (Blum, 2018). Most of the functional properties of a half-sarcomere unit at the filament level can be scaled up to represent muscle tissue at large (McMahon, 1984; Zajac, 1989). While this approach may discount certain mechanical properties that contribute to muscle behaviors, such as links between sarcomeres (Campbell, 2009), this model allows us to isolate specific cross-bridge dynamics in order to characterize their effect on force production in a muscle.

The user inputs to the simulations are activation and length, represented as the fraction of activated actin binding sites, f_{act}, and the length change per time step of the total half-sarcomere unit, respectively. The model has the capability of controlling the activation through calcium concentrations. However, for simplicity, the thin filament activation is decoupled from these chemical changes and controlled directly by the user control. The input length is defined as the command length, L_{cmd}. This value may not always align with the actual half-sarcomere length, L_{hs}, such as when the model experiences behaviors that cause it to fall slack. Slack occurs when the muscle is shortened too quickly or reaches lengths that cannot be sustained by the filament properties. In this situation, when L_{cmd} does not equal L_{hs}, the model enters a slack mode in

which the cross-bridge distribution is allowed to evolve and then the model uses the distribution and forces to iteratively search for the new half-sarcomere length. This process is repeated until the half-sarcomere length is once again less than or equal to the command length (Blum, 2018).

For the most part, the model operates in "length control" mode where the command length is equivalent to the half-sarcomere length and the user controls the behaviors directly through the activation and length inputs. The model then proceeds through a series of operations to generate cross-bridge behaviors and subsequently evaluate forces. The first step is updating the fraction of activated actin binding sites and the half-sarcomere length within the model according to the input driver. Next, the length of the half-sarcomere, or the command length, is used to determine or update the overlap between the thick and thin filaments. Third, the thin filament properties are updated. This step is redundant when f_{act} is being controlled directly, but allows for control of activation through calcium concentrations within the model. In the fourth step, the myosin head population is allowed to evolve over time. Finally, the change in length is applied to the population of myosin heads in order to shift their distribution (Blum, 2018).

The fraction of overlap represents the fraction of myosin heads that overlap with the thin filament. This is determined by the filament parameters as well as the input length of the half-sarcomere from the second step. The thick filament has a given total length, which includes "bare zone" where there are no myosin heads. Thus, the maximum length of overlap, $L_{max\ overlap}$, that is available for binding is actually the thick filament length, $L_{thick\ filament}$, minus the bare zone length, $L_{bare\ zone}$. The fraction of overlap, $f_{overlap}$, is represented as:

(1) $$f_{overlap} = \frac{L_{thin\ filament} + L_{thick\ filament} - L_{hs}}{L_{max\ overlap}},$$

where the numerator represents the interfilamentary overlap by adding the total length of the thin filament, $L_{thin\ filament}$, plus the total length of the thick filament, $L_{thick\ filament}$, minus the half sarcomere length, L_{hs} (Blum, 2018). This value is divided by the maximum length of overlap in order to determine the fraction of overlapping myosin heads available for attachment. Therefore, as the half-sarcomere contracts and the length decreases, the amount of overlap between the filaments increases. The maximum of this value is set to 1 to accommodate for when the thin filament overlaps past the myosin head population and into the bare zone. In this situation, the numerator would be greater than the denominator, but the overlap of the myosin heads has already reached 100%, so this overlap value is capped. It also has a set limit of zero in case the half-sarcomere length is moved below the thin filament length of the model. In the current version of this model, the thin filament length $L_{thin\ filament}$ is 1120 nm and the thick filament length $L_{thick\ filament}$ is 815 nm. The bare zone length on the thick filament is 80nm (Blum, 2018). Therefore, maximum overlap occurs between half-sarcomere lengths of 1120 nm, when the thick filament is fully occluded by the thin filament, and 1200 nm, when the thin filament overlaps the entire section of the thick filament that is not bare.

Once the fraction of activated binding sites on the thin filament is updated in the third operation, the fraction of overlapping myosin heads and the fraction of activated actin binding sites is used to determine the fraction of available binding sites.

(2) $$f_{available}(t) = \min\left[f_{act}(t),\ f_{act}(t) \times f_{overlap}(t)\right] - f_{bound}(t)$$

The fraction of binding sites available for cross-bridge attachment, $f_{available}$, is dictated by the minimum between the fraction of activated binding sites, f_{act}, and the fraction of binding sites

overlapped with myosin heads, $f_{overlap}$, minus the fraction of those already bound in a cross-bridge, f_{bound} (Blum, 2018). Assuming that the actin binding sites are activated uniformly along the thin filament, the fraction of available binding sites due to $f_{overlap}$ is also limited by the activation level. This was a key modification to the active force production within our model. The K. P. Blum model defined this behavior as a function of f_{act} and $f_{overlap}$. However, cross-bridge attachment at non-optimal lengths (i.e. when $f_{overlap}$ is smaller than f_{act} and is the limiting factor of $f_{available}$) is still affected by activation level. This modification allowed the model to exhibit length-dependent and activation-dependent force production within the fibers that varies in response to interfilamentary overlap, as confirmed in previous studies (McMahon, 1984; Stanfield, 2017).

The fourth and fifth operation steps in the model involve the cycling activity of the cross-bridge population. For simplicity, the model consists of a two-state myosin head system for cross-bridge cycling where the state is either defined as attached or detached. The amount of attached and detached myosin heads is determined by a set of partial differential equations that use experimentally determined rates of binding and unbinding. These rates are represented as functions of the cross-bridge length and govern the amount of cross-bridges in the attached and detached states. The thick and thin filaments are dynamically coupled as the number of cycling cross-bridges is determined in their bound state by the thick filament and in their unbound state by the thin filament. Therefore, the model can evolve the cross-bridge population over length and time and use the distribution of cross-bridge lengths to determine active force (Blum, 2018).

The active force is calculated by summing the forces of all the attached myosin heads at a point in time:

(3) Active force = $F_{active} = \int_{-\infty}^{\infty} k_{cb} \rho f(x)(x + x_{ps})dx$

The active force, F_{active}, represents the sum of the cross-bridge forces by multiplying the cross-bridge stiffness, k_{cb}, by the length of the cross-bridge, $x + x_{ps}$, times the cross-bridge density, ρ, multiplied by the fraction of attached myosin heads, $f(x)$, and integrating over all cross-bridge lengths. When a myosin head attaches to an actin binding site, the cross-bridge undergoes a conformational change called a power stroke. This behavior allows the cross-bridge to act like a spring, where the power stroke length, x_{ps}, is added to the length at which the cross-bridge attached, x. In the current version of this model, the cross-bridge stiffness k_{cb} is 1 mN m^{-1}, the cross-bridge density ρ is 6.9 x 10^{16} m^{-2}, and the power stroke length x_{ps} is 2.5 nm (Blum, 2018).

The passive force in this model is determined by multiplying a linear stiffness constant by the length of the half-sarcomere relative to an optimal fiber length, l_0 (Blum, 2018). This approach is consistent with the observations that passive forces are only produced at lengths above or equal to optimal (Zajac, 1989). However, the passive force equation produces a linear force-length relationship that is not consistent with the exponential force generation in resting muscles (McMahon, 1984). Furthermore, the l_0 parameter in the cross-bridge model is used to determine certain slack behaviors that affect the minimum half-sarcomere lengths and the maximum shortening velocities that the model can sustain. Thus, it has effects on both the passive force and the cross-bridge behaviors produced at lengths below "optimal." Since our primary interest is the cross-bridge force generation behaviors, we decided to remove the passive force equation and use this length parameter only for slack to determine minimum lengths that the half-sarcomere can reach. For all stretch simulations, this "slack" parameter is set to 815 nm, the length of the thick filament, and the model does not reach lengths below this value.

Simulations

We reproduced a series of classical muscle experiments to characterize the force generation within the cross-bridge model in comparison to expected results and Hill-type model behaviors. The optimal lengths for the model range from 1120 nm to 1200 nm, where overlap is 100% and the only limiting factor of available binding sites is activation. For the purposes of these simulations, the optimal length, L_0, is defined as the midpoint of this range at 1160 nm. Furthermore, the time vector is shifted so that the time value corresponds to the beginning of each stretch, and any isometric holds prior to movement occur before time zero.

Force-length simulations

In order to characterize the force-length relationship in the half-sarcomere, we conducted simulations following classical force-length experiments (McMahon, 1984; Rack & Westbury, 1969; Zajac, 1989). The simulations consisted of a simple isometric hold with maximal activation. The imposed lengths were normalized to the optimal fiber length 1160 nm. The half-sarcomere model was first fixed at given lengths, varying from 500 nm (<0.5 of the optimal length) to 2000 nm (>1.5 of the optimal length), and then the activation level was set to 1. More simulations were conducted at lengths greater than optimal in order to fully characterize the force-length relationship. In order to give the model time to settle completely, the forces were taken after a 10 second hold, at time point 5 (Figure 1a). These force measurements were compared to the applied command lengths to represent the force-length relationship in the model. The simulations were then repeated with an activation level of 0.5. The Hill-type model from Dr. Gregory S. Sawicki was used to plot the Hill-type parameters for the force-length relationship.

Force-velocity simulations

In order to characterize the force-velocity relationship, we conducted a series of ramp-hold stretches over a fixed optimal length at varying lengthening and shortening velocities. A ramp-hold stretch consists of an imposed length change at a constant velocity followed by a hold period where the muscle is fixed at the given end length. Lengthening velocities were denoted by negative vectors and shortening velocities by positive vectors. The velocities varied from -9280 nm/s to 9280 nm/s, or -8 L_0/s to 8 L_0/s, over a 50 ms stretch duration. The forces were evaluated in the center of the stretch duration when the muscle was being actively lengthened or shortened at a constant velocity. Initial and final lengths were specified to ensure that the same length value was reached at the midpoint of the stretch at time point zero for each simulation (Figure 1b). Therefore, the forces were all taken at the same half-sarcomere length and could be compared to the varying velocities to represent the active force-velocity relationship in the model. Since the length was consistent across simulations, a constant passive force was applied in order to scale the total force and to compare the maximum shortening velocity (i.e. when total force falls to zero) within the model to the Hill-type model. The simulations were repeated with an activation level of 0.5. The G. S. Sawicki Hill-type model was used to plot Hill-type force-velocity relationship.

Half-sarcomere ramp-hold simulations

We also subjected the model to a series of controlled ramp-hold stretches to characterize the response of the half-sarcomere to imposed movements. The first subset of 10 ramp stretches were all performed at the same velocity with varied stretch duration periods in order to reach different final lengths. The half-sarcomere was fully activated, 1, and held isometrically at L_0 for

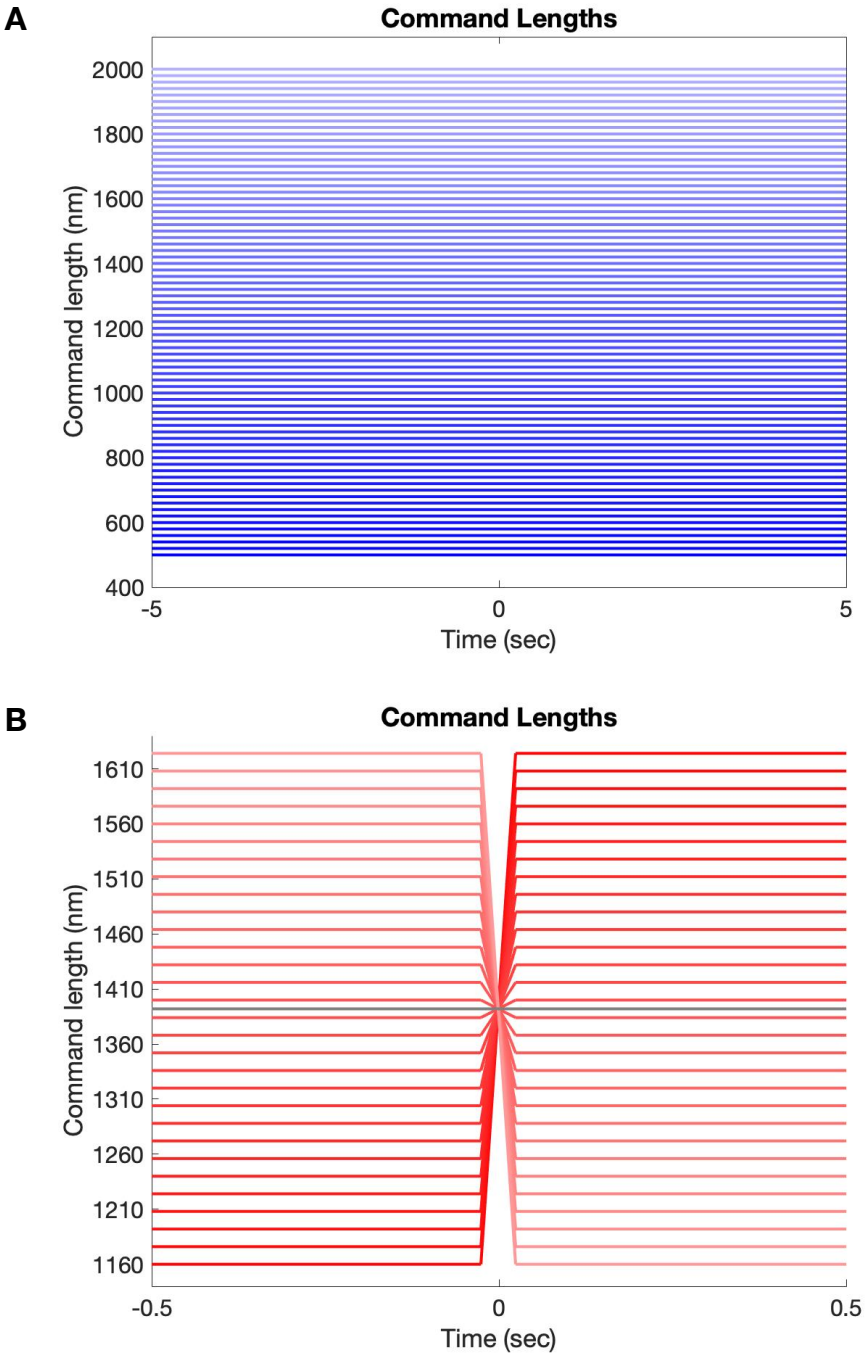

Figure 1. Imposed length changes during force-length and force-velocity simulations. During force-length simulations, the half-sarcomere was fixed at a length and activated fully. The lengths ranged from 500 nm to 2000 nm. During force-velocity simulations, the half-sarcomere was activated fully and then subjected to a ramp stretch at a constant velocity. The velocities ranged from -9280 nm/s to 9280 nm/s and the command length reached 1392 nm at the 0 second time point of each simulation. Forces are normalized to the force produced during the zero velocity simulation at length 1392 nm (grey trace). A) Imposed command lengths across force-length simulations. B) Imposed command lengths across force-velocity simulations.

5 seconds. Following this pre-stretch hold, we applied a stretch at velocity 100 nm/s, or 0.086 L_0/s. The stretch durations between simulations increased linearly from 0.2 seconds to 2 seconds. This guaranteed that the ramp stretches would all be performed at the same constant velocity but would terminate at varying lengths. The ramp stretches were immediately followed by another isometric hold at the new fiber length, which varied linearly from 1180 nm to 1360 nm, or 1.017 L_0 to 1.172 L_0.

The next subset of ramp stretches was designed to reach the same end length with varying ramp stretch velocities. The series of simulations each consisted of an imposed ramp stretch of varying velocities. Different stretch durations were used to ensure that each stretch would end at the same length for the second isometric hold. The activation was set to 1 and the length was fixed at L_0 for a 5 second isometric hold. The imposed stretch durations increased linearly from 1 second to 3 seconds and the stretch velocities varied proportionately from 66.7 nm/s to 200 nm/s, or 0.057 L_0/s to 0.172 L_0/s. The second isometric hold was fixed at length 1360 nm, 1.172 L_0.

Cross-bridge ramp-hold simulations

To confirm the early transient activity first characterized in cross-bridge behavior, we recreated a small-scale stretch experiment performed in real muscle fibers. This experiment consisted of small-scale isotonic contractions of less than 0.5% of the initial length so to produce distortion of the cross-bridge attachments without causing detachment (McMahon, 1984). We applied a series of 10 small ramp-holds. The half-sarcomere was activated fully to produce tension, held at L_0 for 5 seconds, and then rapidly shortened. The magnitude of the shortening was varied from 1 nm to 5nm (less than 0.5% L_0) over a duration of 1 ms. The stretch duration was a key constant during the experimental procedures so to isolate rapid transients in muscle

activity and avoid any slower stabilizing effects or reformation of the cross-bridges (McMahon, 1984).

History-dependence simulations

To confirm the time-history dependent behavior of the model, we reproduced a series of ramp-release simulations used to model the sensitivity of muscle to prior movements (Blum, 2018), scaled to the current model parameters. Each simulation consists of three identical ramp-release stretches, where the muscle is subjected to an imposed ramp stretch of a constant velocity, followed by an immediate release period where the muscle is shortened at the same magnitude velocity. The first two stretches happen successively with no hold in between, with the third occurring after a possible isometric hold at the initial length. Across 11 simulations, the time delay before the third stretch is varied linearly from 0 to 10 seconds. Imposed ramp stretches were performed at a constant velocity of 118.2 nm/s for both lengthening and shortening, each over a 0.6 second time period. The activation was set to 1 and the initial length was set to 1130 nm to ensure that the entirety of the stretch occurred within optimal lengths at maximum activation. This highlights the cycling activity of the cross-bridges by eliminating any limiting effect between filaments, such as overlap and activation, and verifies that every component of the cross-bridge population is available to form connections.

RESULTS

Force-length behavior

The cross-bridge force produced by the model changes in response to changes in the length of the half-sarcomere during isometric holds (Figure 2a). Compared to the ramp-hold stretches, these simulations are regulated to isolate changes in length (i.e. no velocity). The initial phase of the tension responses features a rapid force adjustment in response to the model being activated in the first time step. Each trace reaches a steady-state value within the first second and remains constant for the remainder of the simulation. The active forces do not increase continuously as a passive elastic component would, but instead rise in response to increasing half-sarcomere lengths at lower values, reach a peak, and then begin to drop as lengths continue to increase. Half-sarcomere lengths at the limits of the simulations, at or below 620 nm (0.534 L_0) and greater than or equal to 1940 nm (1.672 L_0), produce a net zero force within the cross-bridges. Maximum forces are reached at lengths at or between 1120 nm and 1200 nm, the optimal fiber lengths of the model (Figure 2a).

Force-velocity behavior

When the length of the half-sarcomere is controlled for, the active force response varies in response to changes in velocity. The force responses during each simulation were recorded at time point zero when the fiber was at the same length but was being subjected to different imposed velocities (Figure 1b). The active force shows an initial scaling to the length of the first isometric hold period. The range of stretches that begin within the range of optimal lengths, 1120nm to 1200 nm, settle to the same maximum isometric force during this phase. In the lengthening simulations, the cross-bridge force increases rapidly at the onset of the stretch.

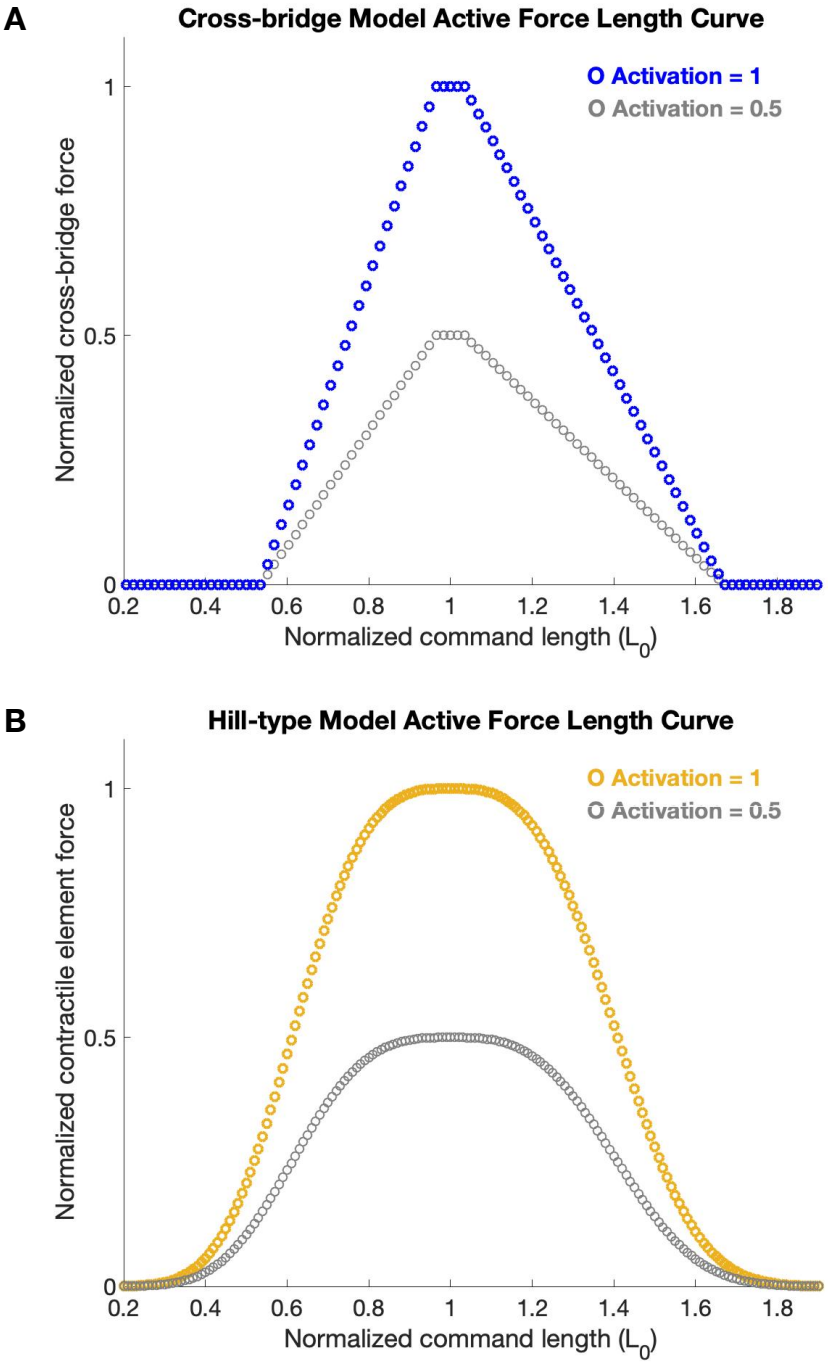

Figure 2. Force-length curves from the cross-bridge model compared to the Hill-type model. During the force-length simulations, active force was evaluated at the end of the isometric hold. The forces from the Hill-type model were plotted as a function of length based on the predetermined force equations. The same simulations with an activation level of 0.5 are plotted in grey. A) Fixed command lengths plotted against active force evaluations from the cross-bridge model. B) Muscle lengths plotted against active force values produced by the Hill-type model.

In the shortening simulations, the cross-bridge forces are more variable, reaching negative tension values within the cross-bridges and exhibiting possible stabilizing behaviors over the course of the length change. The forces at high shortening velocities do not stabilize during the stretch, but return to a stable value at rest.

Force-length and force-velocity relationships

Maximum forces occurred within the optimal lengths of the half-sarcomere and declined at lengths below or above this range (Figure 2a). However, the response to non-optimal lengths was not symmetrical. The ascending limb of the active force-length curve is 47% steeper than the descending limb. Therefore, forces are produced at a greater range of lengths beyond optimal. The maximum force produced scaled proportionately with activation as a function of the equation for available binding sites (Equation 3). During the ascending and descending limb of the force-length curve, the limiting factor of the available binding sites is the amount of overlap between the filaments. However, in the peak of the curve, the limiting factor is activation of the thin filament. When the activation level was set to 0.5, the range of optimal lengths remained constant. However, the maximum forces produced scaled with the activation level to half the value of those produced during the maximal activation condition. The ascending and descending limbs of the force-length curve scaled with activation as well (Figure 2a).

The force-length relationship encoded in the Hill-type model displays a similar maximum at optimal lengths, with forces falling to zero by 0.2 L_0 and 1.9 L_0. Furthermore, the Hill-type model scales with activation in a similar manner. Maximum forces produced at optimal lengths scales proportionately with the activation level, as well as the slopes of the ascending and descending limbs of the curve (Figure 2b).

Maximum forces during imposed velocity simulations occurred during high negative velocities (i.e. lengthening). As the velocity began to approach zero and increase in the positive direction (i.e. shortening), the forces began to decline, sharply at first and more gradually as velocities continued to increase (Figure 3a). The slope was not assumed to be continuous through the force measurement taken at zero velocity (Zajac, 1989). Therefore, the force relationship during lengthening and the force relationship during shortening were plotted as two separate exponential equations. (Figure 3a). At high shortening velocities, cross-bridges began to produce negative forces. With a passive component, this causes the total force to fall to zero at high shortening velocities. The velocity at which total force reaches zero is known as the maximum shortening velocity. The maximum shortening velocity is greater in the cross-bridge model than the Hill-type model. However, both models approach similar maximum force values during lengthening (Figure 3b).

The maximum force during lengthening and the maximum shortening velocity varied with activation in the cross-bridge model (Figure 3a). However, only the maximum force values scaled with activation level in the Hill-type model. The maximum shortening velocity remained constant (Figure 3b).

Forces vary with length and velocity during stretch

The active forces produced by the model vary with length and velocity. The force traces in response to ramp stretches performed at a constant velocity all follow the same values through the duration of the stretch period (Figure 4b). There is a high initial tension response, followed by a more stable phase where the force declines linearly. This is consistent with a biphasic tension response that is determined in its initial phase by movement history and in its latter phase by stretch velocity (Campbell & Lakie, 1998). Once the stretch terminates and the muscle is

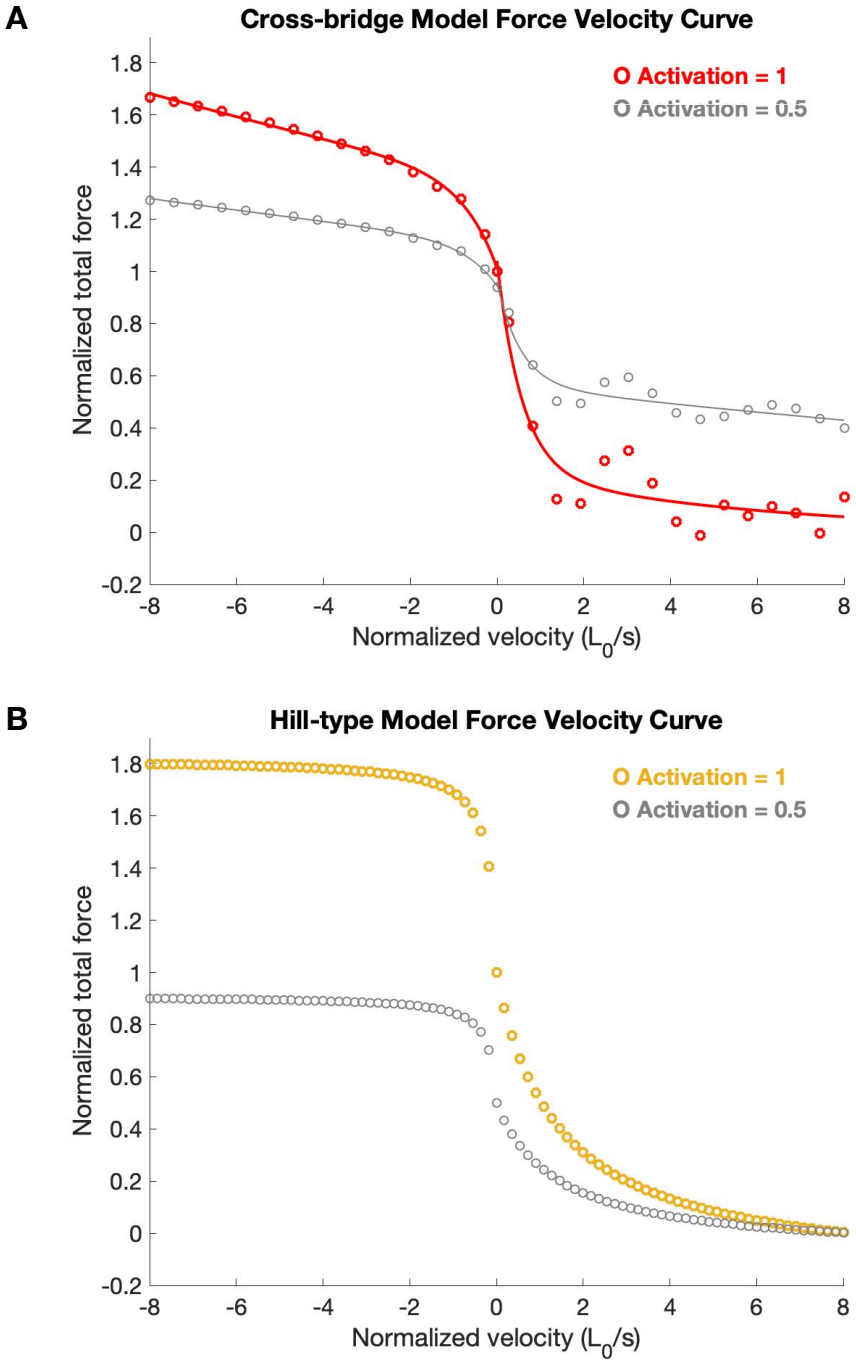

Figure 3. Force-velocity curves from the cross-bridge model compared to the Hill-type model. During the force-velocity simulations, active force was evaluated at the midpoint of the constant velocity stretch. The forces from the Hill-type model were plotted as a function of velocity based on the predetermined force equations. The same simulations with an activation level of 0.5 are plotted in grey. A) Fixed velocities plotted against total force evaluations from the cross-bridge model. B) Velocity plotted against total force values produced by the Hill-type model.

fixed at a given length, the active force falls rapidly until reaching a steady-state value (Figure 4b). This final value of the cross-bridge force scales in response to the half-sarcomere length, with greater half-sarcomere lengths with less filament overlap eliciting lower active force values (Figure 4a & 4b).

The shape of the force response varies with different stretch velocities when the initial and final lengths of the half-sarcomere are held constant (Figure 4d). The maximum value of the cross-bridge force increases as stretch velocity increases. The initial burst before the brief plateau in force also increases relative to the remainder of the force trace in conditions of higher stretch velocities (Figure 4c & 4d). The traces exhibit a similar phase of steady linear decline during the stretch (Figure 4b & 4d). The slope of this phase varies proportionately to stretch velocity (Figure 4d).

Early transients in cross-bridge force

The active force responses to small-scale ramp-hold stretches showed an initial sharp drop in force, the slope of which scaled with shortening velocity. The short duration of the stretch limited the minimum forces reached by the cross-bridges during this phase. Once the muscle reached a constant length, the cross-bridge force featured a rapid recovery period before more gradually approaching a constant value (Figure 5b). The fraction of bound myosin heads did not change during any of the simulations until after the stretch concluded and the cross-bridges began to reform to the new fiber length. Therefore, the initial rapid elastic response seen in the active force is a result of distortion of the cross-bridge attachments. Another emergent property of the active force is that as the tension falls at greater shortening velocities and the model begins to produce negative cross-bridge forces that resist shortening (Figure 5b). The half-sarcomere lengths are consistent with the command lengths throughout each simulation, i.e.

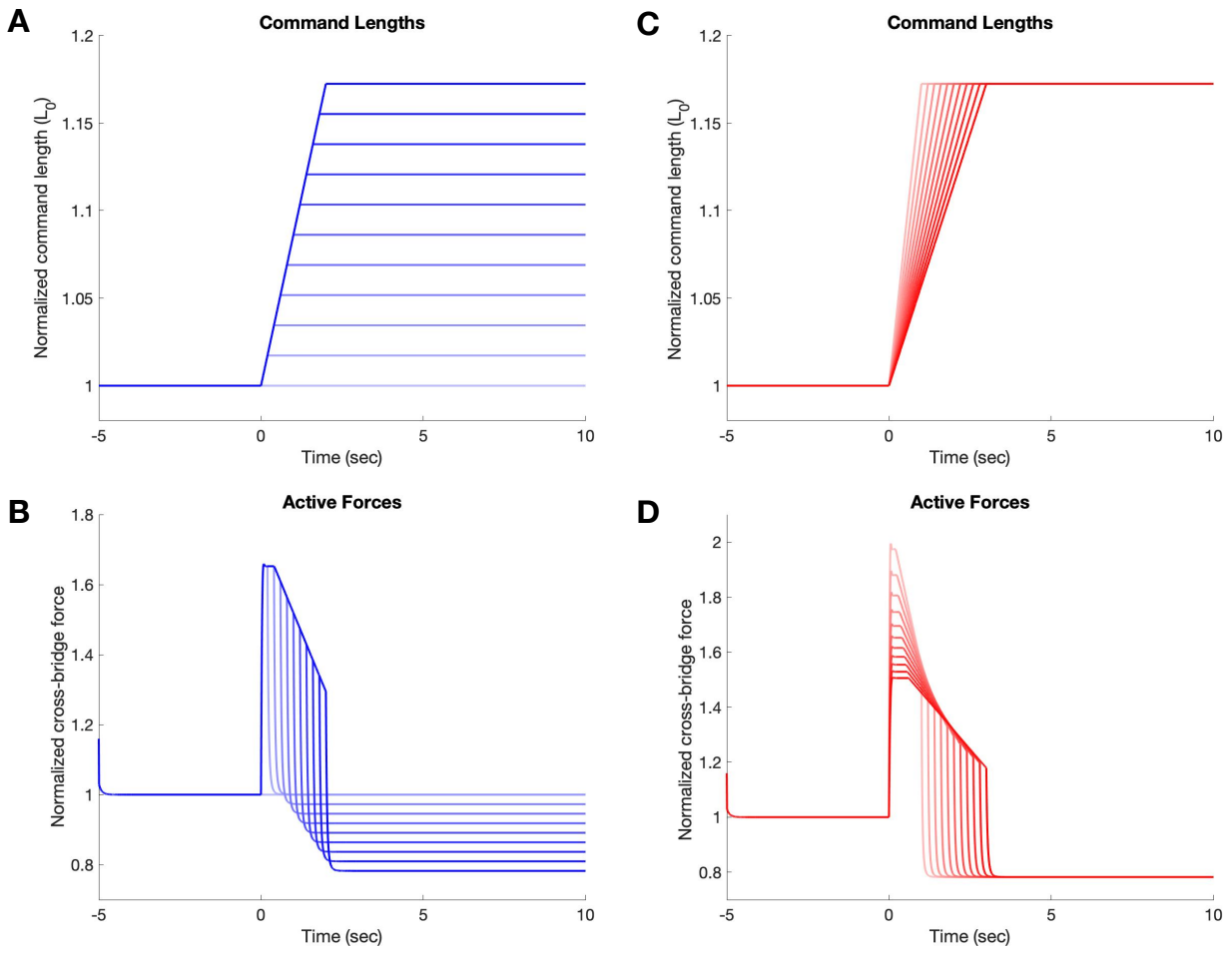

Figure 4. Active force responses to ramp-hold simulations. The activation level was set to 100% in all simulations. Constant velocity simulations were subjected to an imposed stretch at 0.086 L_0/s, beginning at L_0 and terminating at lengths ranging from 1.017 L_0 to 1.172 L_0. Fixed length simulations were stretched from L_0 to 1.172 L_0 at velocities ranging from 0.057 L_0/s to 0.172 L_0/s. A) Imposed command lengths over time during constant velocity simulations. B) Active forces produced across constant velocity simulations. C) Imposed command lengths over time during fixed length simulations. D) Active forces produced across fixed length simulations.

the muscle is never slack. Therefore, the cross-bridges are able to produce negative tension without causing the muscle to fall slack.

History-dependent force generation

The shape of the tension response varied across different rest time intervals. Every simulation began with two ramp-release stretches with no time delay in between them. The

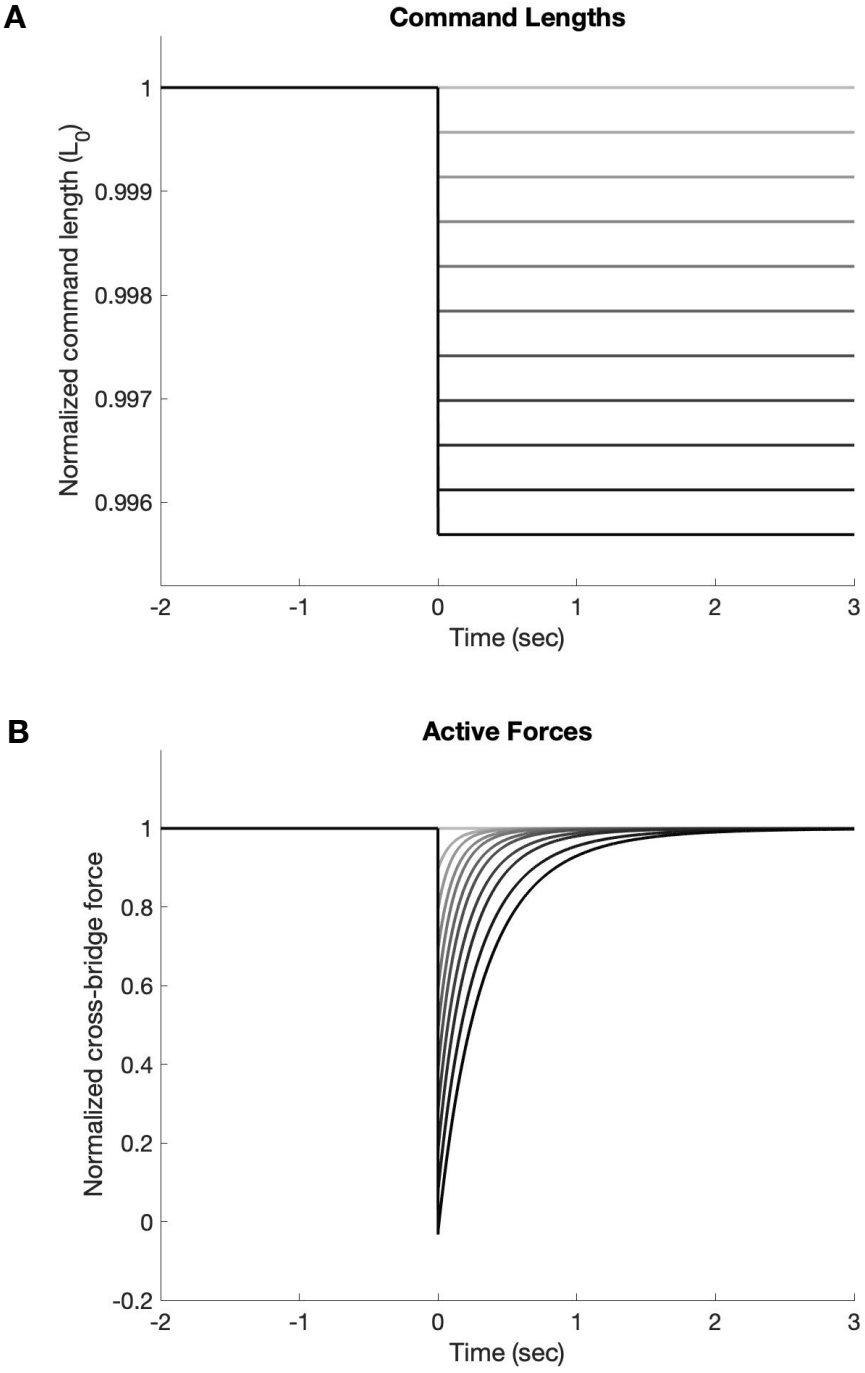

Figure 5. Transient active force responses to small-scale length changes. The model was activated fully and subjected to a length step that decreased the half-sarcomere length. The length changes varied from 1nm to 5 nm (less than 0.5% of the optimal length), each over a duration of 1 ms. A) Normalized command lengths over the duration of the simulation. B) Normalized cross-bridge force in response to the length change.

active force response to the second ramp-release stretch was markedly different than the force generated in response to the first. The first stretch elicited an initial peak in tension that dropped to a relatively stable value for the duration of the lengthening stretch, before falling off as the muscle began to shorten. The second stretch did not elicit an initial peak but featured a more gradual increase of force over the duration of the stretch (Figure 6b). The kinematic features of the imposed third stretch were identical to the first and second, varying only in time delay

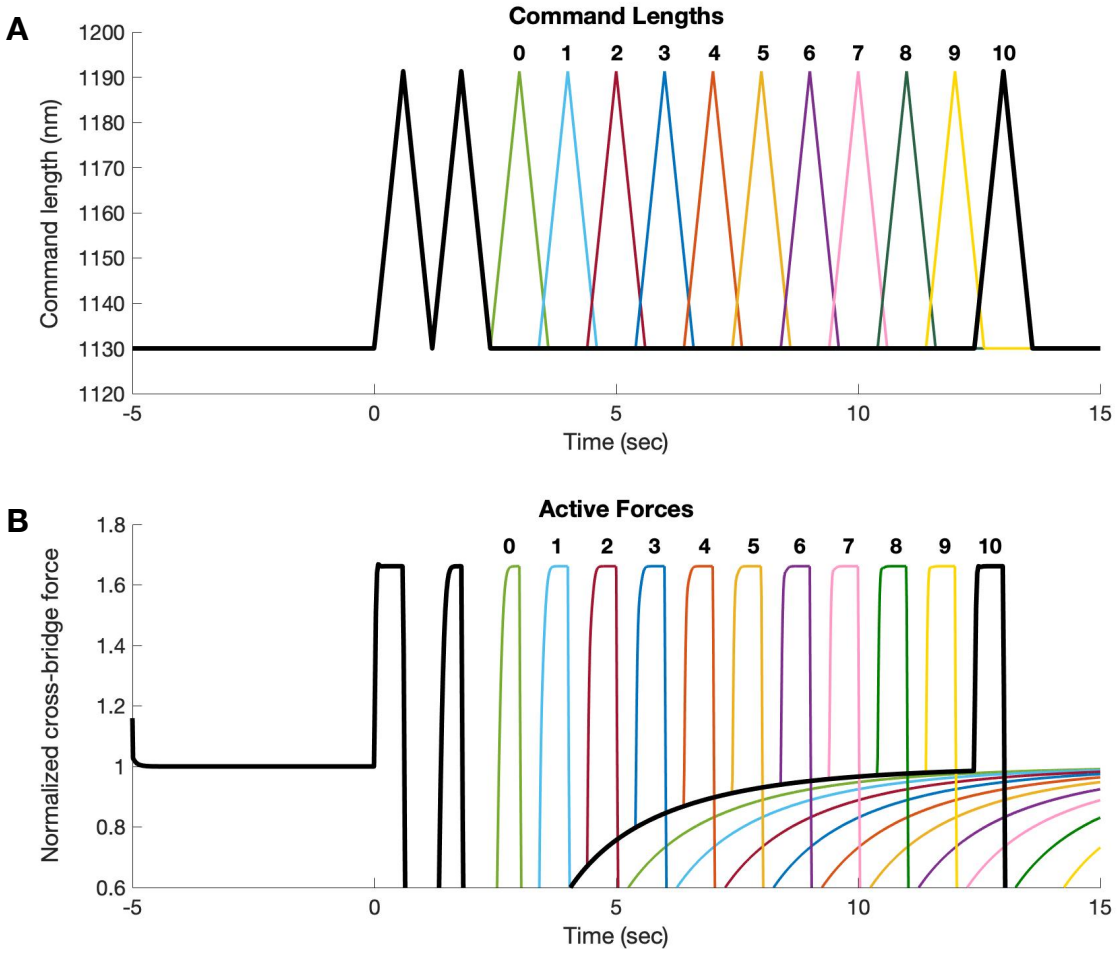

Figure 6. Active force responses to timing of ramp-release stretches. The model was activated fully and subjected to a series of imposed ramp-release stretches, each performed at a speed of 118.2 nm/s for 0.6 seconds. The stretches occurred between 1130 nm and 1190 nm. The first two ramp-release stretches were repeated for every simulation, with the third varying only in onset timing from latency 0 to 10. The time interval between the second and third ramp-release stretch varied from 0 seconds to 10 seconds. The final simulation at latency 10 is traced in black. A) The imposed command lengths of the half-sarcomere. B) The active force produced during ramp-release stretches.

between simulations. When the third ramp-release stretch was performed without any time delay, the cross-bridge force response exhibited the same features as the response to the second (Figure 6, green trace at latency 0). As the time interval between the second and third ramp-release stretches increased, the shape of the force responses gradually regained characteristics of the response to the initial stretch (Figure 6, latencies 1-9). When the third ramp release stretch occurred after a rest period of 10 seconds, the force response was almost identical to first, including the initial peak in tension that was higher than the force produced during the remainder of the stretch (Figure 6, black trace at latency 10). The same magnitude of force was reached in each stretch response. However, the early portion of the response varied across time latencies.

DISCUSSION

Modeling the cross-bridge dynamics has the potential to capture critical features of muscle behaviors during movement. Incorporating history-dependent mechanisms of force generation may help clarify previously unexplained experimental results, as well as help predict patterns of movement and locomotive strategies used during dynamic behaviors. However, we must first characterize the behavior of the cross-bridge model in static conditions in comparison to established models and experimental findings.

The initial step was to confirm the force-length and force-velocity relationships within the model. Hill-type models produce these behaviors through predetermined responses. However, the cross-bridge model intrinsically produces forces, through the cycling activity of the myosin heads, that is dependent on length and velocity. These relationships were found to be consistent with key characteristic of the force-length and force-velocity curves used for Hill-type models (Zajac, 1989). The peak of the force-length curve occurred at optimal lengths of the fiber. Furthermore, the model produced asymmetrical forces in the ascending and descending limbs of the curve, with the force rising more steeply at lengths below optimal. In the force-velocity relationship, the maximum force occurred during lengthening simulations and produced a characteristic sharp decline as shortening velocity increased. When the passive component was included, the total forces also begin to approach a maximum shortening velocity. The scale of this passive force is a focus for future modifications as well as for scaling when examining our model in different simulations.

The modification to the $f_{available}$ equation allowed the active force produced by the model to scale with activation as the Hill-type model predicts. The scaling of the force-velocity curve with activation did not follow the Hill-type behavior. However, this may also be a result

of a passive component influence that is shifting the force-velocity curve in our cross-bridge model.

The next step was to confirm the early transient activity first identified in cross-bridge experiments. The initial elastic response to shortening is consistent with Hill-type models. However, negative forces that resist shortening is a phenomenon that can only occur within the cross-bridges (McMahon, 1984). This behavior has been observed in negative load conditions and is consistent with the idea that cross-bridges form elastic links that can be pulled in the negative direction during high velocities before they are able to detach, temporarily producing forces that resist shortening in muscle (Edman, 2014). This behavior only appears during high shortening velocities and not during any length simulations, supporting the idea that these forces are a product of temporary elastic resistance in the cross-bridges when they are not allowed enough time to detach, instead of a compensatory result of calculating force and slack in the model.

The final step was to confirm history-dependence within the model. The short-range elasticity of the model is the key component of history-dependent force generation. The active force is dependent on prior activation and movement due to the cycling activity of the myosin heads. When a muscle is left at rest, the cross-bridges are able to reform attachments and reach a steady-state where their distribution is centered around cross-bridge length zero. This produces a high initial resistance to stretch. Prior movement that does not allow the cross-bridges to reform should decrease this stiffness in response to stretch (Blum, 2018). We tested the force response of the cross-bridges to movement history. When the model was subjected to a series of identical movements that varied only in onset latency, the patterns of force generation adjusted accordingly. Forces generated after a period of rest featured a rapid elastic response in tension,

whereas prior movement markedly decreased this response. This confirmed the thixotropic property of model that resets the sensitivity of the model to stretch over time.

These simulation results provide a platform for further investigation into dynamic conditions. Characterizing the force responses compared to previous experimental results in static conditions confirms that the model is able to intrinsically produce behaviors we see in muscles, including history-dependent patterns of force generation. Understanding the fundamental behaviors of the model provides to opportunity for integration with movement simulations, as well as helps provide a basis for future modifications.

Our model currently takes the same inputs as the Hill-type model that is used in hopping simulations. We intend to integrate the cross-bridge model into the active component of the Hill-type model through Simulink. This platform will be able to apply the user inputs and then pass the cross-bridge distributions through in order to calculate the active force of the muscle. Furthermore, this will allow us to utilize the passive component of the Hill-type model as well as the series elastic component (i.e. the tendon) in conjunction with the cross-bridge dynamics of our model. The Simulink platform allows us to study work loops as a first step for studying the mechanics of a muscle-tendon unit and the contributions of neural control. Identifying the major neural and mechanical factors in producing cyclic movements is key understanding how a muscle-tendon unit is able to contribute to stable and efficient locomotion. (Sawicki, Robertson, Azizi, & Roberts, 2015). After characterizing the effects of timing and patterns of activation on the muscle-tendon unit, we can move into simulations of steady and perturbed hopping movements, potentially clarifying the effects of history-dependence in producing robust and dynamic responses.

REFERENCES

Blum, K. P., D'Incamps, B. L., Zytnicki, D., & Ting, L. H. (2017). Force encoding in muscle spindles during stretch of passive muscle. *PLOS Computational Biology,* 13(9). doi:10.1371/journal.pcbi.1005767

Blum, K. P. (2018). *A history-dependent model of muscle spindle function*. Unpublished manuscript.

Campbell, K. S., & Lakie, M. (1998). A cross-bridge mechanism can explain the thixotropic short-range elastic component of relaxed frog skeletal muscle. *Journal of Physiology,* 510(3), 941-962. doi:10.1111/j.1469-7793.1998.941bj.x

Campbell, K. S., & Moss, R. L. (2002). History-dependent mechanical properties of permeabilized rat soleus muscle fibers. *Biophysical Journal,* 82(2), 929-943. doi:10.1016/S0006-3495(02)75454-4

Campbell, K. S. (2009). Interactions between connected half-sarcomeres produce emergent mechanical behavior in a mathematical model of muscle. *PLOS Computational Biology,* 5(11). doi:10.1371/journal.pcbi.1000560

Campbell, K. S. (2014). Dynamic coupling of regulated binding sites and cycling myosin heads in striated muscle. *Journal of General Physiology,* 143(3), 387-399. doi:10.1085/jgp.201311078

Dick, T. J., Biewener, A. A., & Wakeling, J. M. (2017). Comparison of human gastrocnemius forces predicted by Hill-type muscle models and estimated from ultrasound images. *Journal of Experimental Biology,* 220(9), 1643-1653. doi:10.1242/jeb.154807

Edman, K. A. P. (2014). The force–velocity relationship at negative loads (assisted shortening) studied in isolated, intact muscle fibres of the frog. *Acta Physiologica,* 211(4), 609-616. doi:10.1111/alpha.12321

Huxley, A. F. (1957). Muscle structure and theories of contraction. *Progress in Biophysics and Biophysical Chemistry,* 7, 255-318.

Libby, T., Chukwueke, C., Sponberg, S. (2019). History-dependent perturbation response in limb muscle. *BioRxiv*. doi:10.1101/509646

McMahon, T. A. (1984). *Muscles, Reflexes, and Locomotion*. Princeton, NJ: Princeton University Press.

Proske, U., & Morgan, D. L. (1999). Do cross-bridges contribute to the tension during stretch of passive muscle? *Journal of Muscle Research and Cell Motility,* 20, 433-442.

Rack, P. M., & Westbury, D. R. (1969). The effects of length and stimulus rate on tension in the isometric cat soleus muscle. *Journal of Physiology,* 204(2), 443-460. doi:10.1113/jphysiol.1969.sp008923

Rack, P. M., & Westbury, D. R. (1974). The short range stiffness of active mammalian muscle and its effect on mechanical properties. *Journal of Physiology,* 240(2), 331-350.

Razumova, M. V., Bukatina, A. E., & Campbell, K. B. (1999). Stiffness-distortion sarcomere model for muscle stimulation. *Journal of Applied Physiology,* 87(5), 1861-1876. doi:10.1152/jappl.1999.87.5.1861

Robertson, B. D., & Sawicki, G. S. (2014). Exploiting elasticity: Modeling the influence of neural control on mechanics and energetics of ankle muscle–tendons during human hopping. *Journal of Theoretical Biology,* 353, 121-132. doi:10.1016/j.jtbi.2014.03.010

Ross, S. A., Nigam, N., & Wakeling, J. M. (2018). A modeling approach for exploring muscle dynamics during cyclic contractions. *PLOS Computational Biology,* 14(4). doi:10.1371/journal.pcbi.1006123

Sawicki, G. S., Robertson, B. D., Azizi, E., & Roberts, T. J. (2015). Timing matters: tuning the mechanics of a muscle–tendon unit by adjusting stimulation phase during cyclic contractions. *Journal of Experimental Biology,* 218, 3150-3159. doi:10.1242/jeb.121673

Stanfield, C. L. (2017). *Principles of Human Physiology* (6th ed.). Pearson.

Voloshina, A. S., Kuo, A. D., Daley, M. A., & Ferris, D. P. (2013). Biomechanics and energetics of walking on uneven terrain. *Journal of Experimental Biology*, 216, 3963-3970. doi:10.1242/jeb.081711

Zajac, F. E. (1989). Muscle and tendon: Properties, models, scaling, and application to biomechanics and motor control. *Critical Reviews in Biomedical Engineering,* 17(4), 359-411.